

METALS IN THE INTERGALACTIC MEDIUM⁴BASTIEN ARACIL¹, PATRICK PETITJEAN^{1,2}, CHRISTOPHE PICHON³ AND JACQUELINE BERGERON¹*Submitted*

ABSTRACT

We use high spectral resolution ($R = 45000$) and high S/N ratio (40-80 per pixel) spectra of 19 high-redshift ($2.1 < z_{\text{em}} < 3.2$) quasars to investigate the metal content of the low-density intergalactic medium using pixel-by-pixel procedures. This high quality homogeneous survey gives the possibility to statistically search for metals at H I optical depths smaller than unity. We find that the gas is enriched in carbon and oxygen for neutral hydrogen optical depths $\tau_{\text{HI}} > 1$. We do not detect C IV absorption statistically associated with gas of $\tau_{\text{HI}} < 1$. In addition, our observations strongly suggest that the C IV/H I ratio decreases with decreasing τ_{HI} . We observe that for $\tau_{\text{HI}} \sim 1$, $\log \text{C IV/H I} < -3.2$. This does not prevent a small fraction of this gas from being associated with strong metal lines as a probable consequence of the IGM enrichment being highly inhomogeneous. We detect the presence of O VI down to $\tau_{\text{HI}} \sim 0.2$ with $\log \text{O VI/H I} \sim -2.0$. We show that O VI absorption in the lowest density gas is located within $\sim 400 \text{ km s}^{-1}$ from strong H I lines. This suggests that this O VI phase may be part of winds flowing away from overdense regions. There is no O VI absorption, at $\tau_{\text{HI}} < 1$, associated with gas located at velocities larger than $\sim 400 \text{ km s}^{-1}$ away from strong absorption lines. Therefore, at the limit of present surveys, the presence of metals in the underdense regions of the IGM is still to be demonstrated.

Subject headings: *Cosmology: observations – Galaxies: haloes – Galaxies: ISM – Quasars: absorption lines*

1. INTRODUCTION

One of the key issues in observational cosmology is to understand how and when star formation took place in the high redshift universe. In particular, it is not known when the first stars appeared or how they were spatially distributed. The direct detection of these stars is challenging and the intergalactic medium (IGM) provides a record of stellar activity at these remote times. Indeed, metals are produced in stars and expelled into the IGM by supernovae explosions and subsequent winds and/or by galaxy interactions. It is therefore crucial to observe the distribution of metals present in the IGM at high redshifts.

The high-redshift IGM is revealed by numerous H I absorption lines observed in the spectra of remote quasars (the so-called Lyman- α forest). It has been shown that at $z \sim 3$, C IV absorption is seen to be associated with most of the strong H I absorption lines ($\log N(\text{H I}) > 14.5$; Cowie et al. 1995; Tytler et al. 1995) that are believed to trace dense filaments connecting massive haloes where the stars can naturally form (e.g. Cen et al. 1994, Petitjean et al. 1995, Hernquist et al. 1996, Bi & Davidsen 1997).

The question of whether the gas filling the underdense space (the so-called voids) delineated by these overdense structures also contains metals or not is crucial. Indeed, it is improbable that winds from star-forming regions

located in the filaments can pollute the voids (Ferrara et al. 2000). Therefore, if metals are found in the gas filling the voids, they are likely to have been produced in the very early Universe by objects more or less uniformly spatially distributed.

Cowie & Songaila (1998) introduced a method to measure the mean C IV optical depth corresponding to all pixels of the Lyman- α forest with similar H I Lyman- α optical depth (see Aguirre et al. 2000, for an extensive discussion of the method). They showed that the mean C IV optical depth correlates with τ_{HI} for $\tau_{\text{HI}} > 1$. Ellison et al. (2000) used the same method on a spectrum of very high signal to noise ratio and concluded that there is some amount of carbon in the low density gas. However, in their data, C IV is only detected in gas with $\tau(\text{H I}) > 1$. Data are inconclusive for $\tau(\text{H I}) < 1$ (see Schaye et al. 2003). Schaye et al. (2000) applied the method to search for O VI and claimed to have detected O VI in gas of mean H I Lyman- α optical depth as low as 0.1. We have applied the method introduced by Cowie et al. (1995), and slightly modified, to a set of homogeneous data of very high quality obtained during the ESO-VLT Large Programme “QSO Absorption Lines”. Section 2 describes the data and Section 3 the method. Results are presented in Section 4.

2. OBSERVATIONS AND DATA HANDLING

The ESO-VLT Large Programme “QSO absorption lines” has been devised to gather a homogeneous sample of lines of sight suitable for studying the Lyman- α forest in the redshift range 1.7–4.5. High resolution ($R \sim 45000$), high signal-to-noise ratio (40 and 80 per pixel at, respectively, 3500 and 6000 Å) UVES spectra have been obtained over the wavelength ranges 3100–5400 and 5450–9000 Å. Although a large emission redshift range is covered, $2.2 < z < 4.5$ (see Table 1), em-

¹ Institut d’Astrophysique de Paris – CNRS, 98bis Boulevard Arago, F-75014 Paris, France; name@iap.fr

² LERMA, Observatoire de Paris-Meudon, 61 avenue de l’Observatoire, F-75014 Paris, France

³ Observatoire de Strasbourg, 11 rue de l’Université, 67000 Strasbourg, France

⁴ Based on observations collected at the European Southern Observatory (ESO), under the Large Programme ”QSO Absorption Line Systems” ID No. 166.A-0106 with UVES on the 8.2m KUEYEN telescope operated at the Paranal Observatory, Chile

TABLE 1
LIST OF LINES OF SIGHT

Name	z_{em}	Coverage ^a		
		Forest	C IV	O VI
HE1341–1020	2.135	1.55–2.10	2.02–2.10	2.00–2.10
Q0122–380	2.190	1.59–2.16	2.07–2.16	2.05–2.16
PKS1448–232	2.220	1.59–2.19	2.07–2.19	2.05–2.19
PKS0237–23	2.222	1.55–2.19	2.02–2.19	2.00–2.19
HE0001–2340	2.263	1.55–2.23	2.02–2.23	2.00–2.23
Q0109–3518	2.404	1.59–2.37	2.07–2.37	2.05–2.37
Q1122	2.410	1.55–2.38	2.02–2.38	2.00–2.38
HE2217–2818	2.414	1.55–2.38	2.02–2.38	2.00–2.38
Q0329–385	2.435	1.55–2.40	2.02–2.40	2.00–2.40
HE1158–1843	2.449	1.55–2.41	2.02–2.41	2.00–2.41
HE1347–2457	2.611	1.55–2.58	2.02–2.58	2.00–2.58
Q0453–423	2.658	1.59–2.62	2.07–2.62	2.05–2.62
PKS0329–255	2.703	1.62–2.67	2.11–2.67	2.09–2.67
Q0002–422	2.767	1.63–2.73	2.12–2.73	2.10–2.73
HE0151–4326	2.789	1.63–2.75	2.12–2.75	2.11–2.75
HE2347–4342	2.871	1.87–2.83	2.40–2.83	2.38–2.83
HE0940–1050	3.084	1.96–3.04	2.51–3.04	2.49–3.04
Q0420–388	3.117	2.09–3.08	2.67–3.08	2.64–3.08
PKS2126–158	3.280	2.04–3.24	2.60–3.24	2.58–3.24

^aThe upper limit is the emission redshift shifted by 3000 km s^{−1}. The lower limits for the different redshift coverages (respectively, the forest, C IV and O VI coverages) are the minimal observable redshift (due to instrumental limitation or the presence of a Lyman limit break) for Lyman α , Lyman β and O VI respectively. Lyman β is used for the C IV coverage to be sure that the H I optical depth associated to C IV is derived from at least to Lyman series lines.

phasis is given to lower redshifts to take advantage of the very good sensitivity of UVES in the blue and of the fact that the Lyman- α forest is less blended and therefore easier to analyse. In particular, metal lines and amongst them the important O VI transitions, can be more easily detected.

Details of data reduction, normalisation of the spectra and automatic identification of metal lines will be described elsewhere. It is important for this paper to note that great care has been exercised when normalising the spectra. An automatic procedure estimates iteratively the continuum by minimising the sum of a regularisation term and a χ^2 term, which is computed from the difference between the quasar spectrum and the continuum estimated during the previous iteration. Absorption lines are avoided on the basis of the estimate of the continuum. We have carefully calibrated this procedure using simulated spectra of quasars (with emission and absorptions) adding continuum modulations to mimic an imperfect correction of the blaze along the orders and noise to obtain a S/N ratio similar to that in the data. We noted that the procedure underestimates the true continuum in the Lyman- α forest by a quantity depending smoothly on the wavelength and the emission redshift and amounting to about 2% at $z \sim 2.3$. We have obtained this quantity from simulations and corrected the data accordingly. We have used nineteen lines of sight that are described in Table 1 in which we give the name of the objects, the emission redshifts and the redshift coverage along each line of sight for H I Lyman- α , C IV and O VI. The mean redshift of the survey is approximately $z \sim 2.6$.

3. METHOD

Once the Lyman- α forest is cleaned from all metals (see below), the H I Lyman- α optical depth is calculated in each pixel of the forest. When the Lyman- α line is sat-

urated, other transitions in the Lyman series are used. For each Lyman- α pixel, the observed optical depth in the metal transition at the same redshift is measured (see section 3.3). Pixels in the Lyman- α forest are then sorted according to their Lyman- α optical depth and are gathered in optical depth bins that contain a large number of pixels (at least 1000 in the high optical depths bins but as large as 20000 in the low optical depth bins). The median of the associated metal optical depths is calculated in these bins. The median is chosen instead of the mean to avoid biasing the measurement due to a few pixels with high optical depth.

3.1. Determination of τ_{HI} and cleaning the Lyman- α forest from metals

To estimate the Lyman- α optical depth in one pixel, we have to take into account that the absorption optical depth in any pixel can be due to several H I Lyman transitions at different redshifts and also to possible metal lines associated with strong systems. We do this by using all observed transitions in the Lyman- α series. The Lyman- α optical depth in the considered pixel is taken to be the smallest of the τ_{series} that are larger than the noise rms at the corresponding position in the spectrum. This procedure allows us (i) to estimate the optical depth even if a transition is saturated; (ii) to avoid part of the blending effects and (iii) to clean the Lyman- α forest from most of the polluting strong metal absorptions. Indeed, the strong metal absorptions are left over once the H I absorptions have been subtracted.

3.2. Cleaning the spectra

The spectra have been scrutinised to flag all portions of the lines of sight where strong metal lines hide the information we need. These regions and their complements (O VI and H I wavelength ranges in the forest, C IV wavelength ranges in the red) are removed from the analysis. This includes in particular strong Fe II and Mg II systems and all associated systems. When in doubt, we have kept the absorptions (see e.g. Fig. 1). In any case, this means that the C IV and O VI optical depths we derive could be slightly overestimated although we are confident that enough care has been exercised and no obvious system has been missed. We have also restricted the analysis to absorptions located at least 3000 km s^{−1} away from the emission redshifts.

3.3. Metal optical depth

Once the optical depth in the Lyman- α forest, τ_{HI} , is known, the corresponding optical depth of associated metal transitions at the same redshift can be derived. To avoid the effects of blending, we use doublets such as C IV $\lambda\lambda 1548,1550$ and O VI $\lambda\lambda 1031,1037$ to secure the C IV and O VI optical depths. For each of the doublets, the first line has an oscillator strength twice larger than the second line and its true optical depth must be twice larger. We therefore can impose that the two optical depths be consistent.

4. RESULTS

4.1. Presence of CIV

We plot in Fig. 2 the median of the C IV optical depth versus the median of the H I optical depth for the whole

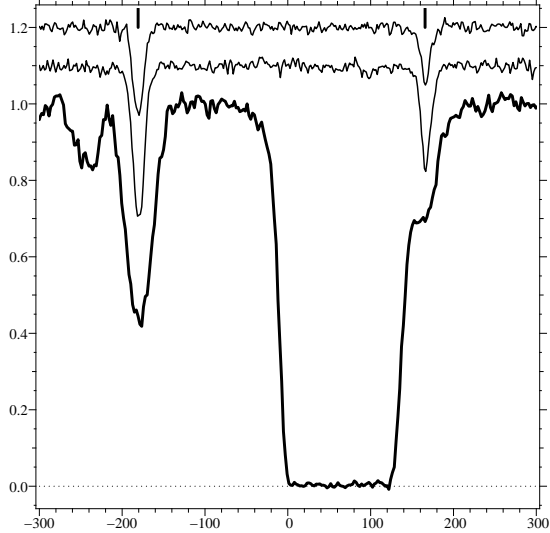


FIG. 1.— Portion of the spectrum of HE 0151–4326 showing a strong Lyman- α absorption line with no C IV absorption associated but two satellite weak H I absorptions have strong associated C IV absorptions.

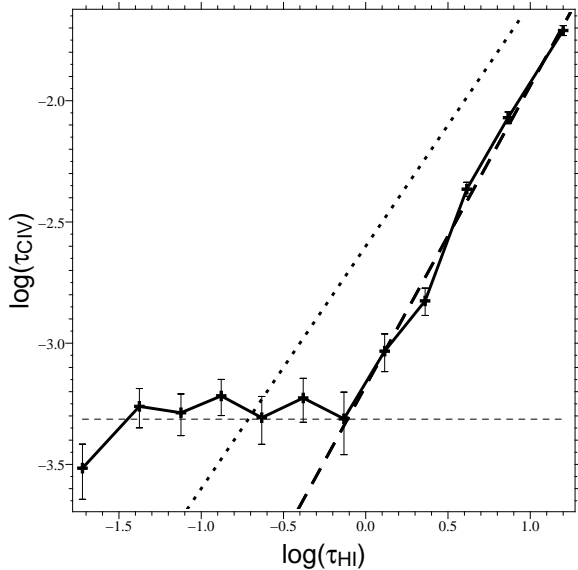


FIG. 2.— Median of C IV optical depth versus median of H I optical depth. Only pixels with velocity difference larger than 3000 km s^{-1} compared to the emission redshift of the quasar are used. The dotted line corresponds to the previous finding by Ellison et al. (2000) ($\log \text{C IV/H I} \sim -2.6$). The dashed thick line is a fit to the data for $\log \tau_{\text{HI}} > 0$: $\log \tau_{\text{CIV}} = 1.3 \times \log \tau_{\text{HI}} - 3.2$. The horizontal dashed line corresponds to the median of τ_{CIV} for $\log \tau_{\text{HI}} < -1.3$.

sample. It can be seen that there is an excess of C IV for $\tau_{\text{HI}} > 1$. For $\tau_{\text{HI}} < 1$, there is no detection of C IV. In particular, the apparent optical depth is statistically the same and consistent with zero for all the bins corresponding to $\log \tau_{\text{HI}} < 0$.

The thick dashed line corresponds to a fit to the data for $\log \tau_{\text{HI}} > 0$: $\log \tau_{\text{CIV}} = 1.3 \times \log \tau_{\text{HI}} - 3.2$. This is steeper than what has been found using Q 1422+230 only (Ellison et al. 2000, Schaye et al. 2003). The dotted diagonal line is the fit by Ellison et al. (2000): $\log (\text{C IV/H I}) = -2.6$. It can be seen that the diagonal line is rejected by our data. Indeed, the present data are inconsistent with a uniform distribution of C IV in the

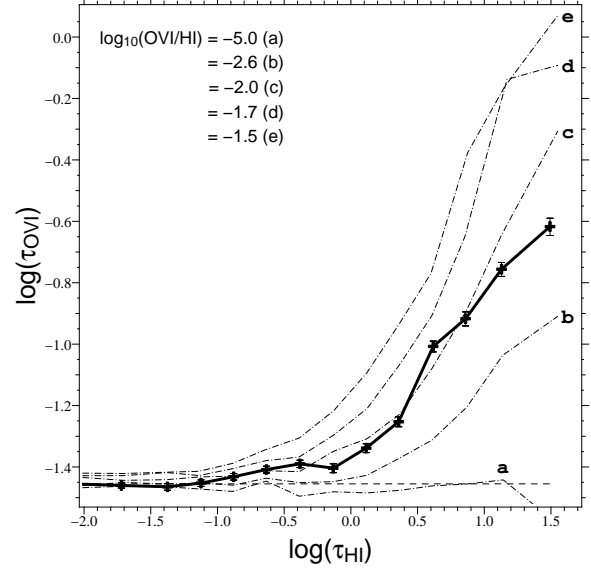


FIG. 3.— The median O VI optical depth is plotted versus the median H I optical depth. The crosses are the observed data, other curves are simulations where the ratio $\log \text{O VI/H I}$ is given fixed values, -5.0 (no metals), -2.5 , -2.0 , -1.7 , -1.5 from the curve labelled (a) to the one labelled (e), respectively

Lyman- α forest with constant C IV/H I ratio. On the contrary our results strongly suggest that the C IV/H I ratio decreases with decreasing τ_{HI} . It is also apparent that for $\log \tau_{\text{HI}} \sim -0.2$, $\log (\text{C IV/H I}) < -3.2$. This is consistent with the value found by Schaye et al. (2003). It is important to note also that the scatter in the C IV optical depth is very similar at different H I optical depths. This means that although the mean C IV optical depth decreases with decreasing τ_{HI} , large C IV optical depths can be seen at nearly any H I optical depth. This is illustrated in Fig. 1 where a strong Lyman- α system is seen with no C IV absorption associated down to our detection limit $\sim 10^{12} \text{ cm}^{-2}$, but two satellite H I weak absorptions have strong associated C IV absorptions (see also Bergeron et al. 2002).

4.2. Presence of OVI

Schaye et al. (2000) performed a similar pixel-by-pixel search for O VI absorption in eight high-quality quasar spectra spanning the redshift range $z = 2.0\text{--}4.5$. In the redshift range $2 < z < 3$, they claimed to detect O VI in the form of a positive correlation between the H I Lyman- α optical depth and the optical depth in the corresponding O VI $\lambda 1031$ pixel, down to $\tau_{\text{HI}} \sim 10^{-1}$. On the contrary, they did not detect O VI at $z > 3$ and considered this as consistent with the enhanced photoionisation from a hardening of the UV background below $z < 3$ although this could also be caused by the high level of contamination from Lyman series lines.

It can be seen from Fig. 3 that our data confirm the detection of O VI down to $\tau_{\text{HI}} \sim 0.2$ that is at smaller H I optical depth than for C IV which is seen down to $\tau_{\text{HI}} \sim 1$ only. To investigate if the signal for $0.2 < \tau_{\text{HI}} < 1$ comes from all parts of the spectrum however, we have divided the sample into two subsamples. The first subsample contains all H I pixels located within Δv from a strong absorption with $\tau_{\text{HI}} > 4$ and the second subsample contains all other pixels varying Δv . It can be

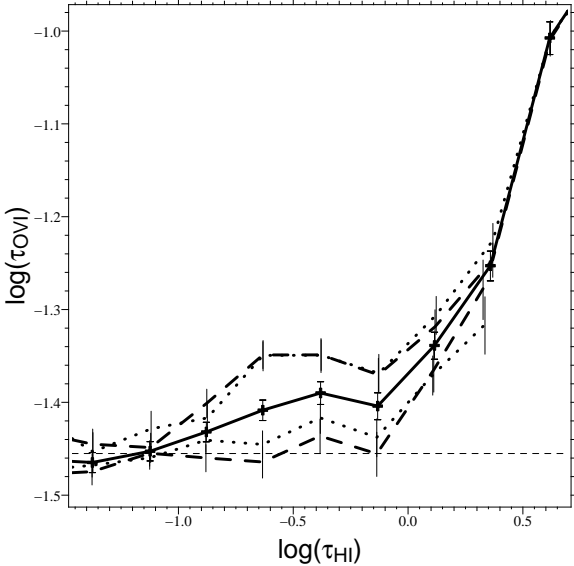


FIG. 4.— Median O VI optical depth versus median H I optical depth for all the data (black curve), for pixels located at less than 500 km s^{-1} (upper dashed curve) or less than 300 km s^{-1} (upper dotted curve) from strong absorptions ($\tau_{\text{HI}} > 4$) and for pixels located at more than 500 km s^{-1} (lower dashed curve) or more than 300 km s^{-1} (lower dotted curve) from strong absorptions.

seen on Fig. 3 that for $\Delta v \geq 300 \text{ km s}^{-1}$, the signal significantly increases for the first subsample. This means that O VI is predominantly seen in the vicinity of strong Lyman- α absorption lines. Indeed, the signal disappears for the second subsample; there is no O VI absorption for $0.2 < \tau_{\text{HI}} < 1$ in the gas. This strongly suggests that the O VI absorption is mostly associated with the surrounding of strong lines probably because the O VI phase is part of winds flowing away from overdense regions. To derive a quantitative limit on the amount of O VI present in the IGM, we have performed simulations of the metal enrichment of the Lyman- α forest. Artificial spectra are created drawing absorption lines at random from a population with column density and Doppler parameter distributions consistent with those observed (Petitjean et al. 1993, Kim et al. 2000). The number of lines is adjusted so that the mean absorption of the simulated spectra is the same as the observed one. A constant O VI/H I ratio is assumed and O VI absorption is added accordingly. Noise consistent with the data is added and the whole procedure described in Section 3 is applied to the simulated spectra. Results are plotted in Fig. 4. It can be seen that data are consistent with $\log \text{O VI/H I} \sim -2$.

5. SUMMARY

We have used a pixel-by-pixel analysis to investigate the presence of metals in the inter galactic medium. We have measured the median optical depth of C IV $\lambda 1548$ and O VI $\lambda 1031$ absorptions versus the H I Lyman- α optical depth of the gas at a mean redshift $z = 2.6$ using 19 lines of sight observed at high spectral resolution ($R = 45000$) and high and homogeneous S/N ratio (approximately 40 and 80 per pixel over, respectively, the O VI and C IV wavelength range). Great care has been exercised to determine the continuum.

We have carefully determined the H I optical depth by taking into account the information in the Lyman series (usually Lyman- β and Lyman- γ). We have also carefully removed from the spectra all wavelength ranges that are polluted by strong intervening absorptions from metal line systems, in particular Mg II and Fe II systems, and from associated systems.

We find that the gas is enriched in carbon and oxygen for $\tau_{\text{HI}} > 1$. Contrary to previous claims, there is no indication that C IV absorption is statistically associated with gas of H I Lyman- α optical depth smaller than 1. In addition, our observations strongly suggest that the C IV/H I ratio decreases with decreasing τ_{HI} . We observe that for $\tau_{\text{HI}} \sim 1$, $\log \text{C IV/H I} < -3.2$. This does not prevent a small fraction of this gas from being associated with strong metal lines. We detect the presence of O VI for $\tau_{\text{HI}} > 0.2$, consistent with a constant ratio $\log \text{O VI/H I} \sim -2.0$. We show that for $0.2 < \tau_{\text{HI}} < 1$, the O VI absorption is associated with gas located within $\sim 400 \text{ km s}^{-1}$ from strong H I lines. This suggests that the O VI phase is probably part of winds flowing away from overdense regions.

It is therefore not possible to conclude that metals are present in the low density regions of the IGM ($\tau_{\text{HI}} < 1$ corresponding to overdensities of about 1 to 3 at $z \sim 2$ and 3 respectively) far away from overdense regions. In particular, it is apparent that at $z \sim 2$, in most of the volume of the Universe, $\log \text{C IV/H I} < -3.2$ and $\log \text{O VI/H I} < -2$. It is therefore probable that the mean metalicity of this gas is smaller than the usual $10^{-2.5}$ solar metalicity derived for clouds with $\log N(\text{H I}) > 14.5$ (see also Schaye et al. 2003). In addition the enrichment of the IGM seems strongly inhomogeneous even at $z = 2$.

We are grateful to the ESO support astronomers who performed the observations in service mode. We thank Evan Scannapieco and R. Srianand for useful comments on the manuscript.

REFERENCES

Aguirre, A., Schaye, J., & Theuns, T. 2002, ApJ, 576, 1
 Bergeron, J., Aracil, B., Petitjean, P., & Pichon, C. 2002, A&A, 396, L11
 Bi, H., & Davidsen, A. F. 1997, ApJ, 479, 523
 Cen, R., Miralda-Escudé, J., Ostriker, J. P., & Rauch, M. 1994, ApJ, 437, L9
 Cowie, L. L., Songaila, A., Kim, Tae-Sun, & Hu, E. M. 1995, AJ, 109, 1522
 Cowie, L. L., Songaila, A. 1998, Nature, 394, 44
 Ellison, S. L., Songaila, A., & Pettini, M. 2000, AJ, 120, 1175
 Ferrara, A., Pettini, M., & Shchekinov, Y. 2000, MNRAS, 319, 539
 Hernquist, L., Katz, N., Weinberg, D. H., & Miralda-Escudé, J. 1996, ApJ, 457, L51
 Kim, T.-S., Carswell, R. F., Cristiani, S., D'Odorico, S., & Giallongo, E. 2002, MNRAS, 335, 555
 Petitjean, P., Mücket, J., Kates, R. E. 1995, A&A, 295, L9
 Petitjean, P., Webb, J. K., Rauch, M., Carswell, R. F., & Lanzetta, K. 1993, MNRAS, 262, 499
 Schaye, J., Aguirre, A., Kim, T. S., Theuns, T., Rauch, M., & Sargent, W. L. W. 2003, astro-ph/0306469
 Schaye, J., Rauch, M., Sargent, W. L. W., & Kim, T. S. 2000, ApJ, 541, L1
 Tytler, D., Fan, X. M., Burles, et al., 1995, QSO Absorption Lines, Proceedings of the ESO Workshop, ed. G. Meylan. Springer-Verlag Berlin Heidelberg New York. ESO Astrophysics Symposia, p. 289